2017

Optimizing riboflavin/ultraviolet-a corneal collagen cross-linking for the treatment of progressive keratoconus

BOSTON UNIVERSITY

SCHOOL OF MEDICINE

Thesis

OPTIMIZING RIBOFLAVIN/ ULTRAVIOLET-A CORNEAL COLLAGEN CROSS-LINKING FOR THE TREATMENT OF PROGRESSIVE KERATOCONUS

by

DANIEL J. SYLVESTRE

B.A., Boston University, 2013

Submitted in partial fulfillment of the

requirements for the degree of

Master of Science

2017

Approved by

First Reader _____

Gwynneth D. Offner, Ph.D.
Director M.S. Medical Sciences Program,
Associate Professor of Medicine

Second Reader _____

Carl Franzblau, Ph.D.
Professor of Biochemistry

OPTIMIZING RIBOFLAVIN/ ULTRAVIOLET-A CORNEAL COLLAGEN CROSS-LINKING FOR THE TREATMENT OF PROGRESSIVE KERATOCONUS

DANIEL J. SYLVESTRE

ABSTRACT

Patients with keratoconus exhibit a biomechanically weakened cornea which loses its proper shape and thereby loses its refractive power. It is usually progressive, beginning with poor visual acuity and eventually necessitating corneal transplant. The cause is likely multifactorial, but involves the weakening of the collagen structure of the corneal stroma, resulting in characteristic thinning and conical distortion. Collagen cross-linking is the first treatment to demonstrate efficacy in halting the progression of the disease. UVA radiation is used to activate riboflavin and photochemically induce cross-linking reactions among collagen and proteoglycans within the stroma, thereby stiffening and strengthening the tissue, and preventing further loss of shape. The current standard treatment, which gained FDA approval less than one year ago, has proven to be efficacious, but has been modified very little since pioneering experiments. Optimization aims to maximize clinical effect while maintaining safety and reducing total treatment time. Major procedural modifications involve

increasing light intensity over a reduced exposure duration, and varying the method of delivering riboflavin to the stroma. Theoretical modeling, informed by and scaled to experimental results, has the potential to predict clinical effect as a function of treatment parameters, enabling tailoring of individual treatments to the specific needs of each patient.

TABLE OF CONTENTS

TITLE i

COPYRIGHT PAGE ii

READER APPROVAL PAGE iii

ABSTRACT iv

TABLE OF CONTENTS vi

LIST OF FIGURES viii

LIST OF ABBREVIATIONS ix

INTRODUCTION 1

Anatomy of the Healthy Cornea 2

Collagen of the Corneal Stroma 8

Collagen Formation 8

Types of Stromal Collagens 16

Macroscopic Organization of Stromal Collagen 20

Keratoconus 23

Signs and Symptoms 23

Diagnosis 24

Etiology/ Risk Factors 26

Review of Major Treatments Prior to CXL 29

Contact Lenses 29

Surgery 30

CXL....33
Effects 38
Current Standard Procedure: Avedro's KXL System 41
MAJOR PROPOSED PROCEDURAL MODIFICATIONS....44
Irradiance.... 44
Modeling 47
Riboflavin Delivery 48
CONCLUDING REMARKS....50
Summary 51
REFERENCES....53
CURRICULUM VITAE....67

LIST OF FIGURES

Figure	Title	Page
1	Light Micrograph of the Human Cornea	4
2	Collagen Synthesis	12
3	Collagen Cross-linking: Lysyl Oxidase	14
4	Orientation of Lamellae in the Posterior Cornea	22
5	Example of Pentacam	25
6	The Molecular Structure of Riboflavin	34
7	Absorption Spectrum of Riboflavin	36
8	Photochemical Reaction Pathways of RFUVA CXL	37

LIST OF ABBREVIATIONS

A-CXL ..... accelerated cross-linking (greater intensity, shorter duration)

AGE ..... advanced glycation end-product

AOPP ..... advanced oxidative protein products

BCVA ..... best corrected visual acuity

COL ..... collagenous domain of collagen

NC ..... non-collagenous domain of collagen

CS/DS ..... chondroitin/dermatan sulfate

CXL ..... corneal collagen cross-linking

ECM ..... extracellular matrix

FACIT ..... fibril-associated collagen with interrupted triple helix)

GAG ..... glycosaminoglycan

HHL ..... histidine-hydroxylysininorleucine

ICRs ..... intracorneal rings

KC ..... keratoconus

KS ..... keratan sulfate

KXL ..... the current treatment system for implementing CXL, created by Avedro

LOX ..... lysyl oxidase

MMP ..... matrix metalloprotease

OCT ..... optical coherence tomography

PG ..... proteoglycan

PLA-CXL ..... pulsed light accelerated cross-linking

RFUVA ..... riboflavin and ultraviolet-A (photo-oxidative cross-linking)

ROS..... reactive oxygen species

S-CXL..... standard cross-linking

SLRP ..... small leucine-rich proteoglycan

INTRODUCTION

The cornea is a transparent structure forming the anterior portion of the eye. It is simultaneously responsible for protecting the eye from mechanical and infectious insult and, together with the tear film, providing roughly 74% of the average eye's 58.6 diopter total refractive power. [1] The specific organization of the its cellular and extracellular components impart the cornea's mechanical integrity, and abnormalities therein can lead to distortion of the cornea's shape, resulting in failure to properly refract light for optimal visual acuity (refractive error).

Keratoconus is a relatively common degenerative condition marked by progressive thinning of the cornea (ectasia) which causes it to bulge outward in a conical shape. The resulting decline in visual acuity may be compounded by scarring and other complications. It typically presents in early adulthood, and is believed to be the result of a combination of genetic and environmental factors. Mild cases may only cause poor visual acuity and astigmatism (a deviation from spherical curvature, which prevents light rays from meeting at a common focus), correctable with glasses or contact lenses. More severe cases eventually require corneal transplant (keratoplasty). Keratoconus is the single most common reason for keratoplasty in the developed world. Research has demonstrated that progression of keratoconus can be halted by photodynamic therapy using

ultraviolet light and riboflavin as a photosensitizer to induce corneal collagen cross-linking.

This introduction will focus on the structural organization of the cornea as it pertains to its mechanical integrity, factors contributing to the loss of said integrity in keratoconus, and the most commonly employed treatments available prior to the FDA approval of Riboflavin/UV-A induced corneal collagen cross-linking (CXL). The following discussion will compare the current protocol for CXL (Avedro's KXL system), with a few proposed procedural modifications which hope to optimize this promising but still nascent treatment.

Anatomy of the Healthy Cornea

The average adult cornea's diameter is approximately 10.5 mm vertically and 11.5 mm horizontally. The average radius of curvature of the anterior surface of the central cornea is 7.8 mm. It is about 0.5 mm thick at the central apex, and gradually thickens to about 0.7 mm toward the periphery where it is limited by the limbus, the border between the cornea and the sclera (the white of the eye). The cornea is both avascular and devoid of lymphatic drainage, and relies on diffusion of nutrients from the aqueous humor - glucose, amino acids, ascorbic acid, other vitamins, and lactic acid – and oxygen indirectly from the air via the tear film. Despite being avascular, the cornea is extremely sensitive, with a density of nerve endings approximately 300 times that found in skin. Innervation

originates from the nasociliary nerve of the ophthalmic division of the trigeminal nerve. [1] In the region of the limbus, the corneal epithelium becomes continuous with that of the bulbar conjunctiva, a thin mucous membrane which covers the anterior part of the sclera. The sclera provides the attachment points for the recti muscles which move the eye. It is at these insertions that the anterior ciliary arteries, which stem from the ophthalmic artery and provide blood supply to the anterior segment, emerge. As shown in Figure 1, there are five recognized corneal layers: epithelium, Bowman's layer, stroma, Descemet's membrane, and endothelium. Posterior to the corneal endothelium is the anterior chamber, the fluid-filled space between the cornea and the iris (the colored portion of the eye surrounding the pupil).[2]

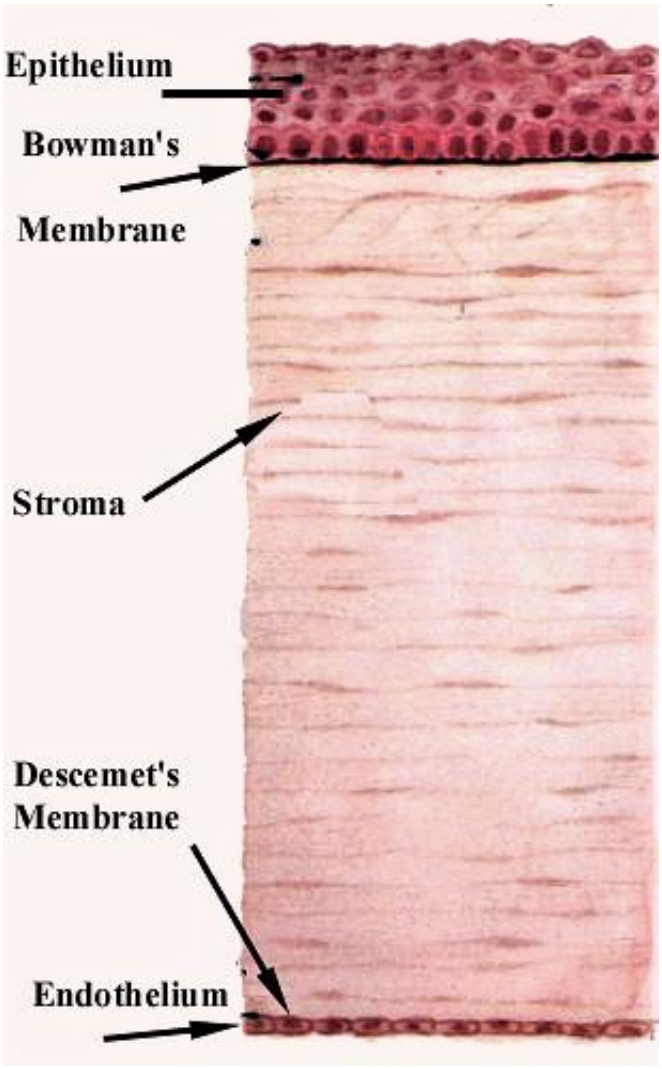

Figure 1: Light micrograph of the human cornea. [3]

The corneal epithelium is composed of extremely uniform stratified squamous non-keratinized cells 4-6 layers totaling approximately 43 μm in thickness. [4] It consists three different types of epithelial cells: superficial, wing, and basal cells. With an average cell lifespan of 7-10 days, deeper basal cells constantly divide and move apically to replace desquamating superficial cells,

resulting in a complete turnover of the epithelium every week. [5] Cells in the outermost layer maintain complexes of tight junctions between them to prohibit tears or foreign chemicals from entering the intercellular spaces. Zonulae adherens and desmosomes are present in all layers of the corneal epithelium, but gap junctions which allow small molecules to pass between neighboring cells are only found in the wing and basal cell layers. Superficial cells project numerous apical microvilli to increase the cell surface area for contact with the tear film. The glycocalyx of these cells provide anchorage for the tear film via association with its inner mucinous layer, which functions to improve the wetting properties of the tears and is produced by goblet cells in the conjunctival epithelium. The middle aqueous layer of the tear film is produced by lacrimal glands around the eye. It allows for even spreading of the tear film over the cornea with each blink, and contains electrolytes, proteins, lysozyme, immunoglobulins, glucose, and dissolved oxygen from the atmosphere, all necessary for proper nourishment of the cornea. The outermost lipid layer is produced by the meibomian glands (modified sebaceous glands) of the eyelid margins. It helps maintain the column of tears between the upper and lower lids, and slows the rate of evaporation of water from the corneal surface. [2] Thus, a healthy tear film allows for a smooth surface for the passage of light, protects it from microbial, chemical, or foreign body assault, and brings nourishment to the avascular cornea including immunological and growth factors which are critical to epithelial proliferation and repair. [6] If the epithelium is damaged, epithelial stem

cells localized to the basal layer of the limbus migrate to the central cornea, differentiating into transient amplifying cells (capable of multiple but limited division), and basal cells. [7] The early nonmitotic coverage phase begins within minutes and can proceed at a remarkable rate, upwards of 70 μm per hour. [8] 24-30 hours later, the basal cells, transient amplifying cells, and limbal stem cells begin mitosis to replenish the cell population. Type IV collagen and laminin secreted by the basal cells are the major components of the epithelial basement membrane, which separates the epithelium from the underlying Bowman's layer, with type VII collagen anchoring fibrils passing between them to provide adhesion of basal cells to the basement membrane and to the stroma. Damaging the basement membrane can prolong epithelial healing to weeks as opposed to days. [1,9]

Technically not a membrane, Bowman's layer is the anterior-most portion of acellular stroma, made up of collagen fibrils (primarily types I and III) and proteoglycans about 17 μm thick. Its precise role is still unclear, although it may help the cornea maintain its shape, or provide a simple barrier function. It does not regenerate, and its disruption may lead to scar formation. [1,4]

The stroma constitutes the bulk of corneal tissue, accounting for nearly 86% of its thickness. [4] Keratocytes residing mostly in the anterior corneal stroma are the major cell type and are responsible for secreting the collagen,

proteoglycans, and matrix metalloproteases (MMPs) which constitute the stromal extracellular space. Collagen accounts for 70% of the total dry weight of the cornea. Corneal collagen forms fibrils with a uniform diameter of approximately 30 nm, which are arranged into larger fibers or lamellae 1-2 μm thick and anywhere from 10 to 200 μm in length, allowing them to traverse the entire cornea from limbus to limbus. [10] The distances between fibers is identical (approximately 42 nm) and their direction in any given lamella is the same, but oriented at a right angle to those of adjacent lamellae. The precise organization of these fibers is the main determinant of corneal transparency, and provides the structural foundation which dictates the cornea's overall shape and biomechanical strength. [1,11] A detailed description of the organization and properties of stromal collagen will be presented in the next section.

Descemet's membrane is the basement membrane of the corneal endothelium. It is constantly secreted by the endothelial cells since before birth and can accumulate up to 10 μm thick with age. It is composed of type VIII collagen and its health is important for the proper exchange of nutrients between the stroma and the anterior chamber. [12]

The corneal endothelium is composed of a single layer of squamous non-keratinized cells having a honeycomb-like mosaic appearance when viewed with specular microscopy. It is approximately 4 μm thick in adulthood. These cells have a high density of ion transport pumps which maintain an osmotic gradient

for fluid flow posteriorly through and out of the corneal stroma, maintaining the stroma in the relatively deturgesced state (78% water content) necessary for its transparency. Cell density of the corneal endothelium is around 3500 cells/ mm^2 at birth and decreases with age at a rate of approximately 0.6% per year. Because of the critical role these cells play in maintaining the water balance of the cornea, a reduction in cell count to below 500 cells/ mm^2 due to age, trauma, inflammation, and other disease processes can result in corneal edema. Remaining cells do have the capacity to “stretch” to fill in the space left by degeneration; however, as this occurs, the remaining cells grow in size (polymegathism) and lose their archetypal hexagonal shape (pleomorphism), both of which are histological indications which correlate to a reduced ability of the endothelium to prevent said edema. [9] These histological correlates allow for the assessment of the health of the endothelium, and thus of the cornea, by specular microscopy.

Collagen of the Corneal Stroma

Collagen Formation

Collagens are trimeric proteins having at least one collagenous or COL domains as well as non-collagenous or NC domains, the number and structure of each depending on the specific collagen type. There are 28 distinct collagen glycoproteins encoded by at least 45 genes designated by Roman numerals (I-

XXVIII) in chronological order of discovery. For each type, each genetically distinct alpha polypeptide chain is designated by Arabic numerals. This discussion will focus only on corneal collagens, specifically those found in the corneal stroma, as this is the primary locus of the effects of photodynamic cross-linking. Figure 2 part A provides an overview illustration of the steps of collagen formation from polypeptide synthesis to fibril assembly.

Collagens I, III, and V form striated fibrils. Unlike I and III, Collagen V retains its N-terminal domain and is involved in the regulation of fibril assembly. Collagen VI forms beaded filaments or networks. There are also collagens that do not form fibrils but are associated with other fibrils, FACITs (fibril-associated collagen with interrupted triple helix). Directed fibril assembly into the highly organized suprastructures observed in tissues such as the cornea depends on cell interaction with the extracellular matrix via organizing molecules such as fibronectin, which itself organizes into a network of fibrils via interaction with integrins. This fibronectin network provides binding sites for collagen fibril assembly. Further assembly of mature fibrils via linear and lateral growth of the preformed intermediates is regulated by small leucine-rich proteoglycans (SLRPs) and FACIT collagens. [13]

Fibril-forming collagens are initially secreted from cells (in the cornea, keratocytes) as procollagens which contain a non-collagenous C-terminal and an N-terminal propeptide, the presence of which prevents premature assembly of

collagen molecules into fibrils inside the cell. Enzymes specific to each collagen type process the propeptides to leave one large central triple helical domain and short non-collagenous end sequences termed telopeptides. For Collagen III and V, this processing can be incomplete, with retention of a C-telopeptide and a partially processed N-propeptide which function as fibrillar assembly regulators.[13]

Collagen molecules are composed of three left-handed helical polypeptide chains within a right-handed superhelix. Initial translation produces pre-pro-peptides which are directed into the lumen of the rough endoplasmic reticulum (RER) of the collagen-secreting cell. Cleavage of the N-terminal signal peptide produces a pro-alpha chain which, after co-translational enzymatic hydroxylation (of prolyl and lysyl residues) and glycosylation of hydroxylysyl residues, trimerize. The hydroxylating enzymes, located either within the lumen or on the inside of the RER, require Fe^{2+}, 2-oxoglutarate, molecular oxygen, and ascorbate as co-factors. Glycosylation of hydroxylysyl residues in collagen requires two enzymes: hydroxylysyl galactosyltransferase, and galactosylhydroxylysyl glucosyltransferase. The extent of glycosylation is collagen type specific and only occurs on non-triple helix substrates (alpha chains). After synthesis is completed, the globular domains fold, stabilized by disulfide bonds, and helix formation begins. Three left-handed coiled alpha chains will supercoil into a right-handed triple helix which is stabilized by inter-chain hydrogen bonds to form the pro-

collagen molecule which exits the cell. Steric hindrance dictates that only glycine can fit in the central position; thus, the triple helical domains have a repeating (Gly-X-Y) pattern, with the X and Y positions usually occupied by proline or lysine residues. Hydroxylation creates two polypeptides unique to collagen, hydroxyproline (the most characteristic amino acid of collagens, important for helix stability), and hydroxylysine (important for down-stream glycosylation). The extent of post-translational glycosylation affects the circumference of the COL triple helical domains and therefore proper fibril assembly. [13]

Once they leave the cell via the Golgi, propeptides are cleaved by proteinases and triple helices self-assemble into a staggered axial array to form microfibrils consisting of five molecules and 4-8 nanometers wide. [14] Different combinations of polypeptide chains (alpha chains) assemble to create different types of collagen, several of which are present in the human cornea. Microfibrils then coil together to form the 30-nm diameter collagen fibril seen in the electron microscope. During fibrillogenesis, parallel collagen molecules are aligned with a small shift to the next (about 25% the length of the collagen molecule) resulting in the classical “quarter-stagger” configuration and the characteristic banded appearance of collagen fibrils under electron microscopy (Figure 2 part B). Because the microfibrils in corneal collagen are tilted about 15 degrees in respect to the fibril long axis, the usual 67 nm axial periodicity, termed the D-period, is reduced to closer to 65 nm and results in a fibril which is narrower than

those found in non-transparent collagen elsewhere in the body such as tendon or sclera which have a more parallel arrangement of microfibrils within them. [15]

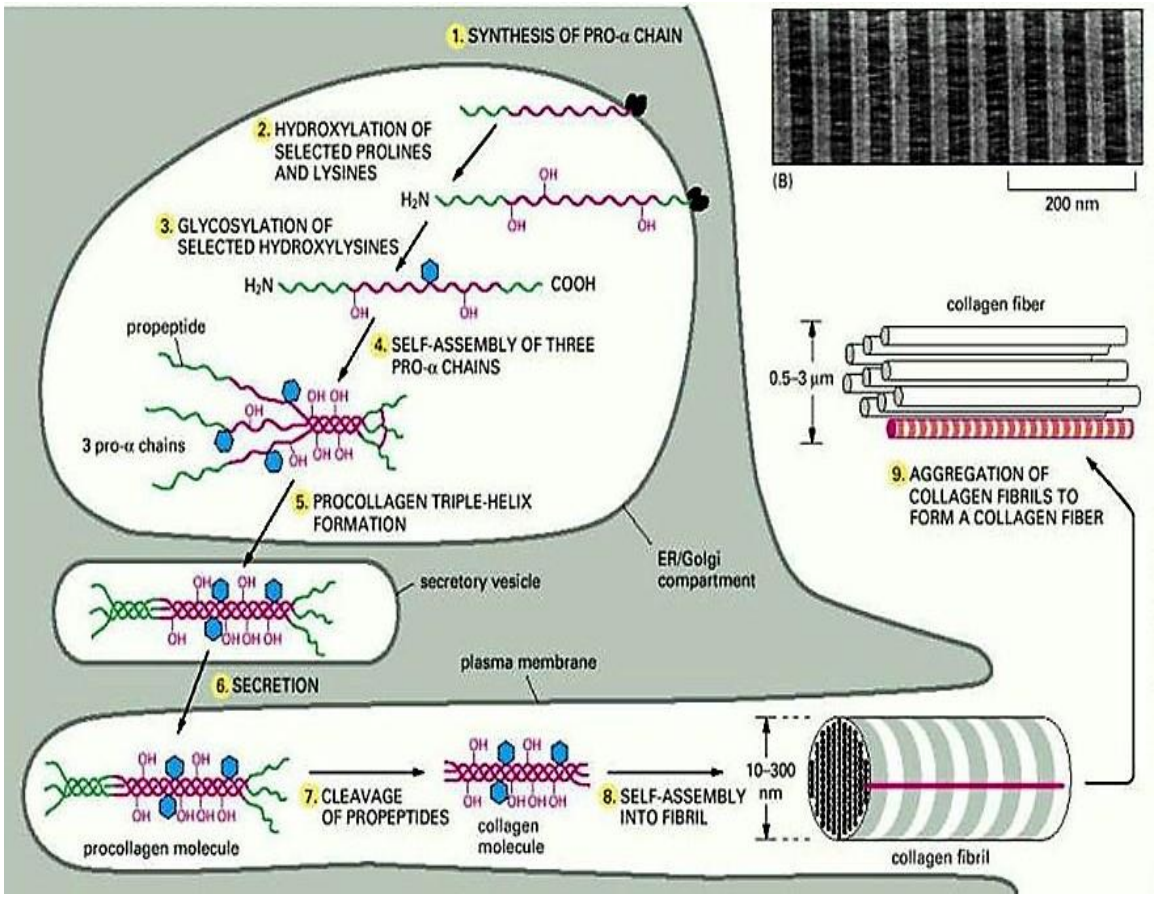

Figure 2: Collagen synthesis (A), and characteristic banded pattern of collagen with electron microscopy (B). [16]

Microfibrils are stabilized by the lysyl oxidase (LOX) enzyme catalyzed intermolecular covalent cross-linking between specific amino acids, mostly modified lysine residues. [17] One amino group within the nonhelical telopeptide is oxidized to form a reactive aldehyde which then bonds to the carbonyl group of

the opposing lysyl residue to produce either an aldimine or keto-imine bond (see Figure 3 below). These bonds can be stabilized by reduction with borohydride to enable isolation and quantification. The type of cross-link is dictated by whether the lysyl residue is hydroxylated, the chance of which is in turn dictated by the level of lysyl hydroxylase in the tissue. Thus, the enzyme that hydroxylates lysine, the long form of lysyl hydroxylase-2, [18] functions as the primary control for the positional pattern of lysyl oxidase-mediated collagen cross-linking. The importance of lysyl oxidase has been demonstrated by its total inhibition in rats treated with β-aminopropionitrile, preventing cross-link formation and resulting in collagen (of aortic tissue in the cited example) lacking tensile strength.[19]

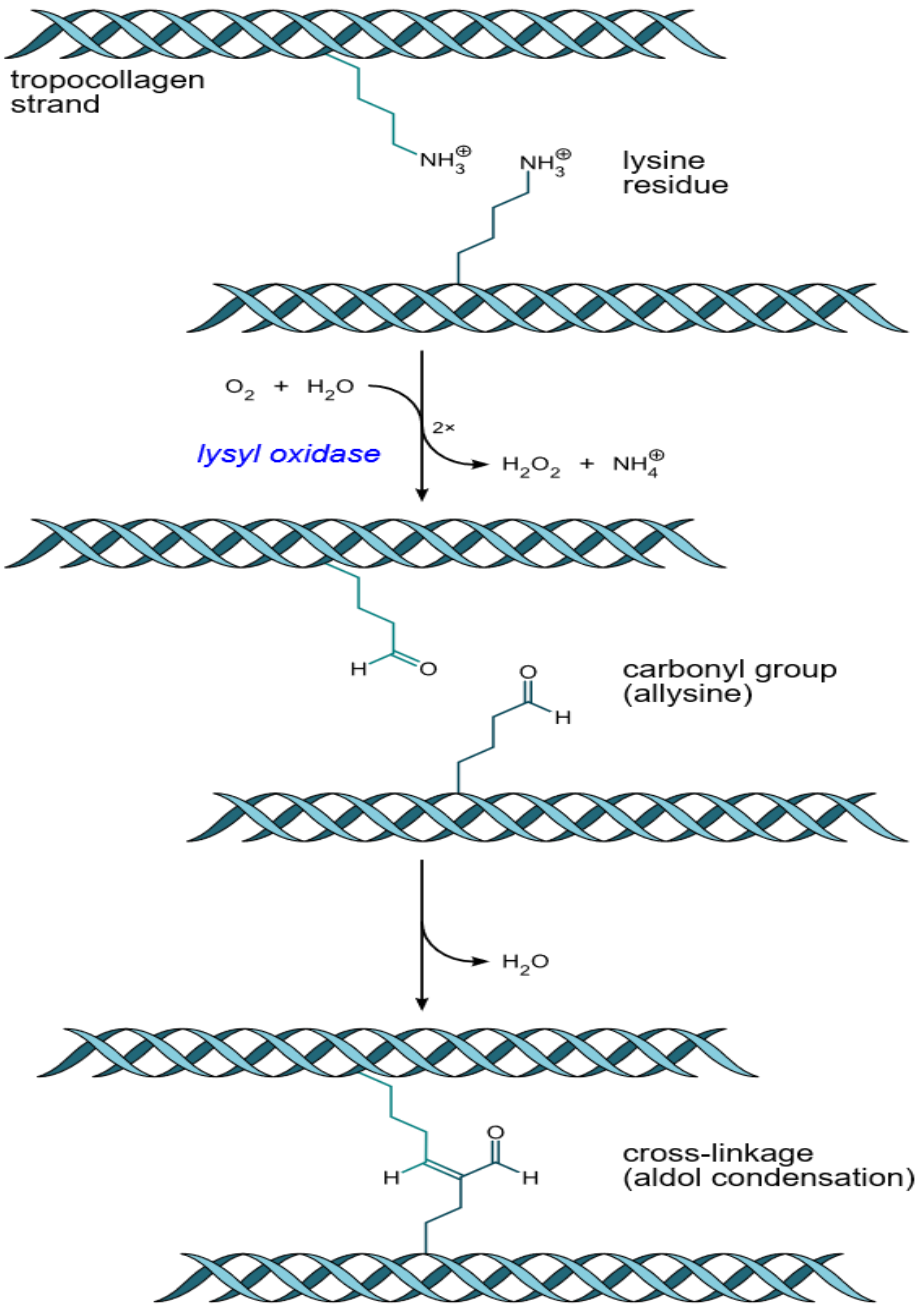

Figure 3: Collagen cross-linking mediated by lysyl oxidase. [20]

The relative proportions of link types are also age-dependent, there being a high proportion of the keto-imine in embryonic corneal collagen and a changeover to only the aldimine in the postnatal cornea. Given that for any given tissue the type of cross-link will be consistent despite there being different types of collagen present, cross-linking appears to be tissue specific rather than specific to collagen type. [21] Although all cross-linking reactions after aldehyde formation occur spontaneously, the highly ordered three-dimensional arrangement of collagen molecules within the assembling microfibril, governed by hydrophobic and electrostatic interactions, facilitates reactions between specific amino acid residues – aldehydes within the C- and N-terminal telopeptides react with lysine or hydroxylysine residues at position 87 and 930 respectively. *In vivo*, the reducible aldimine linkages further react with helical histidine to form the more stable non-reducible HHL (histidine-hydroxylysinonorleucine), cross-links, further stabilizing the fibril network against mechanical stresses. [18,22]

In contrast to enzymatic cross-linking and disulfide bonding, which are normal cross-linking processes tightly controlled by the body for collagen synthesis and tissue organization, non-enzymatic cross-links accumulate in an uncontrolled manner, often having deleterious effects. One such mechanism involves glycation and the products of such reactions, AGEs (advanced glycation end-products). AGEs form as a function of age via the Maillard reaction between

amino acids (especially lysine and proline) and reducing sugars such as glucose. [23] Instead of forming cross-links between telopeptides, these reactions can link helical domains, leading to tissue stiffness and an increased resistance to enzymatic degradation, which disrupts the normal metabolic turnover of collagenous tissue and may lead to fibrosis. [24] However, in KC corneas, this age-related stiffening may be beneficial to the otherwise weak stroma, perhaps explaining the mitigation and eventual cessation of disease progression seen in most patients by the fourth decade of life.

Types of Stromal Collagens

Collagen I is the most abundant of all collagens, found in almost all connective tissues, and representing the greatest proportion of collagens in any given tissue (bone and tendon is 99% Type I). In the cornea, it represents 75% of the collagenous component of the tissue. [25] The triple helix structure of the most common isoform of Collagen I, the type found in the cornea, has the heterotrimeric chain composition α1 $(I)_2$ α2 (I), or two alpha 1 polypeptides twisted together with one alpha 2 polypeptide. [26] This isoform forms heterotypic fibrils with Collagen V, ensuring the regular organization of fibrillar lamellae as well as the unique thinness of each fibril which is crucial for corneal strength and transparency. [27]

Collagen III is a homotrimer composed of three alpha polypeptides. It also associates with Collagen I in heterotypic fibers. Although it is abundant in interstitial tissue reticular fibers (lung, liver, dermis, spleen, blood vessels), as well as elastic tissues, it is weakly expressed in the normal cornea. However, its expression greatly increases in wound healing or inflammation, and is found abundantly in corneal scars. Thus it is considered a principal marker of the stromal matrix remodeling which occurs after corneal injury. [25,28]

Collagen V is relatively abundant in the cornea as compared to other tissues, representing roughly 17% of total collagen content. [25] Collagen V plays a central role in fibril assembly initiation by nucleation, and its N-terminal domain is responsible for regulating fibril diameter. The abundance of Collagen V in the cornea provides many nucleation sites for the assembly of more numerous, smaller-diameter Collagen I fibrils. Furthermore, reducing the amount of Collagen V (e.g. in genetic knockout mouse models), results in fewer fibrils with larger diameters and a disorganized lamellar structure, and loss of corneal transparency. [29,30]

FACITs (fibril-associated collagens with interrupted triple helices) have short COL domains interrupted by NC domains and an N-terminal NC domain which projects into the interfibrillar space. Two C-terminal domains are believed

to interact with collagen I fibrils, and the N-terminal globular domains protrude from the fibril surface, affecting fiber suprastructures and biomechanics.

Proteoglycans are macromolecules containing a protein core with a variable number of glycosaminoglycans (GAGs) attached to it. Collagen fibrils also cross-link non-covalently via interactions with proteoglycans (PGs) and their associated GAGs. These interactions play a crucial role in the spacing of collagen fibers and their orientation, with the length of the GAG-chains dictating the distance between collagen fibrils (interfibrillary distance). [31]

The normal adult human cornea contains the following small leucine-rich proteoglycans (SLRPs): decorin, containing the GAGs dermatan sulphate and chondroitin sulphate (CS/DS), and lumican, keratocan, and mimecan, which contain keratan sulphate (KS) GAGs, the most plentiful corneal GAG. [27] Heparan sulfate proteoglycans are minor components of the cornea and are mainly synthesized by the epithelial cells. [25] SLRP protein cores are synthesized in the rough endoplasmic reticulum and the GAG chains are added in the Golgi, before secretion into the ECM. Defective synthesis of SLRPs causes blindness in humans by disrupting collagen fibril organization. Genetic knockout studies in animals have further affirmed the importance of SLRPs. For example, deficient decorin expression in mice results in fragile skin and dysregulated lateral growth of fibrils. Keratocan knockout results in altered corneal structure, especially

stromal thinning. Human deficiency in keratocan is associated with cornea plana, a congenital condition which causes a decrease in the curvature and therefore refractive power of the cornea, causing symptoms ranging from simple farsightedness to structural malformations and progressive loss of vision in severe cases. [26]

Collagen VI is a nonfibrillar type especially abundant in the cornea. It is characterized by a relatively short triple helical domain and the presence of large globular domains, one of which is a characteristic 140 kDa glycoprotein. It is resistant to degradation by bacterial collagenase, contributing to the immune defense of the eye, and contains numerous inter-chain disulfide bridges which stabilize its tertiary structure. [32] It is typically a heterotrimer of the α1, α2, and α3 chains, with the α3 chain possessing a distinct extended N terminus with an array of consecutive von Willebrand factor type A domains. These specialized domains undergo conformation change and a fraction of them dimerize in the presence of divalent cations. Thus, the conformational state of Collagen VI is substrate specific and will depend on the local charge environment in vivo, modulation of which may reveal or hide binding sites for the numerous other extracellular molecules with which it interacts. [33,34] Because of its large number of potential interactions, collagen VI likely serves as an integrator of the various components of extracellular space with resident cells, a cooperation which is critical to the organized deposition/ assembly of collagen in the ECM.

Collagen VI's supramolecular assembly is different from that of fibrous collagens discussed above. Monomers dimerize in lateral, anti-parallel fashion with C-terminal domains interacting with helical domains and stabilized by disulfide bonds. The resulting overlap creates a 30 nm "stagger" of a central 75 nm supercoiled helical domain flanked by the regions of C then N-globular domains. Still within the cell, dimers align into tetramers which are then secreted and associate end-to-end to form beaded filaments (which then associate laterally to form broad banded fibrils) having a periodicity of approximately 100 nm. Alternatively, tetramers may assemble non-linearly into hexagonal lattices, with the N-termini providing points of interaction with other ECM components. [13] Which suprastructure the tetramers assume is also affected by the imposition of other integrated molecules. For example, SLRPs substituted with dermatan sulfate (DS) chains have been shown to induce hexagonal lattice formation. [35] Within the cornea, the hexagonal lattice arrangement of Collagen I fibers is critical for the transparency of this special tissue. [27]

Macroscopic Organization of Stromal Collagen

As mentioned above, collagen of the corneal stroma is laid down within thin sheets called lamellae, each layer of variable dimensions but typically 1-2 μm thick and up to 0.2 mm broad. Approximately 240 lamellae comprise the thickness of the central human cornea. Anterior lamellae are densely packed,

and highly interlaced, with most of them anchoring their ends into Bowman's layer. These transverse-oriented fibers insert into Bowman's layer at relatively shallow angles, 95% of them within + or – 11 degrees relative to the corneal surface. [11] Increased randomness of angles and branching within the anterior stroma increases tissue stiffness, and a lack of such branching in keratoconus increases corneal compliance and results in a less biomechanically stable anterior cornea more susceptible to interlamellar slippage. [36,37] Moving posteriorly in the central cornea, lamellar packing density decreases, as well as the extent of interlacing, and the degree of hydration increases. The radial orientation of lamellae becomes less random, with a greater proportion arranged orthogonally, pointed in one of two preferred orientations, either the superior-inferior or nasal-temporal directions (see Figure 4). This contrasts with the more isotropic anterior stroma. Among these posterior lamellae, orthogonal preference is gradually lost moving from the central cornea toward the periphery as fibrils adopt an orientation more tangential to the edge of the cornea, eventually forming a circumferential annulus at the limbus. [38–40]

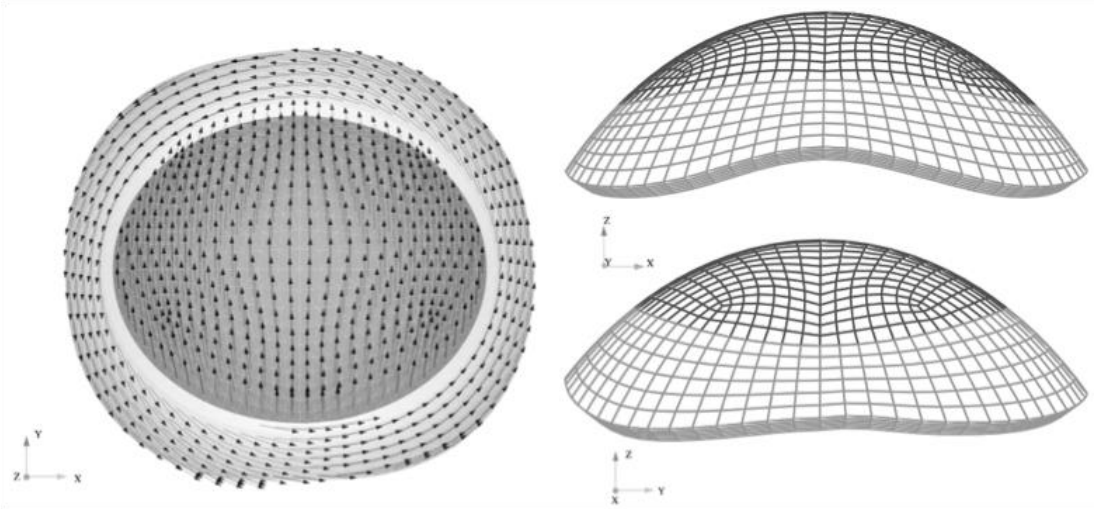

Figure 4: Preferential orientation of lamellae in the posterior cornea. [41]

Being less rigid relative to the anterior cornea, the posterior stroma is more susceptible to edema. Swelling anywhere in the cornea is therefore directed posteriorly and causes a general flattening of the Descemet's membrane. With the limbus providing a structural limit, a flattened Descemet's membrane may crimp into folds at the periphery, creating striae visible upon clinical slit-lamp examination (Vogt's striae). [9] This is a helpful diagnostic criterion for identifying corneal pathology including keratoconus. A prevalence of elastic fibers also exists in the peripheral cornea, which explains the pliability of this region and its ability to absorb intraocular pressure fluctuations, sparing the optically important central cornea from deformation. [42] Finally, so called "anchoring fibers" extend from the limbus to mid-stroma, gradually moving anteriorly before anastomosing with the isotropic anterior collagen fiber network.

These seem to directly connect the anterior central cornea with deeper sclera, further reinforcing it against mechanical distortion. [43] Thus, the macroscopic arrangement of lamellae is critical to the cornea's biomechanical strength and shape-maintenance.

Keratoconus

Signs and Symptoms

The primary symptom of keratoconus (KC) is progressive decline of visual acuity with high, often irregular, astigmatism, which eventually becomes difficult to correct with lenses. Signs include Fleisher's ring - a circular deposition of iron in the epithelium surrounding the base of the cornea, and Vogt's striae - fine vertical lines visible upon slit-lamp examination which are produced by compression of Descemet's membrane. Thinning of the central cornea may be revealed by high-magnification slit-lamp examination, or by ultrasound pachymetry. With further progression, the cornea becomes visibly cone-shaped and produces a V-shaped deformation of the lower lid when the eye looks downward (Munson's sign). Anterior stromal scars may develop due to continuous protrusion of the cornea, especially among patients who wear contact lenses. In some cases, breaks in Descemet's membrane temporarily disrupt the cornea's ability to regulate its hydration and fluid uptake by the overlying stroma results in acute vision loss and pain (corneal hydrops). This usually resolves on

its own after a few days once the membrane regenerates and normal osmotic balance can be restored. [44,45]

Diagnosis

The most sensitive methods for confirming a diagnosis of KC are computerized corneal topography and optical coherence tomography (OCT). The former exploits the principles of Placido disc and Scheimpflug imaging to precisely map curvature of the corneal surface, revealing steepening of the inferior cornea, irregular astigmatism, and other tell-tales. Anterior segment OCT (e.g. Pentacam, as illustrated by Figure 5), provides imagery of the cornea in cross-section, with measurement of corneal curvature and steepness as well as thickness at all locations. [46]

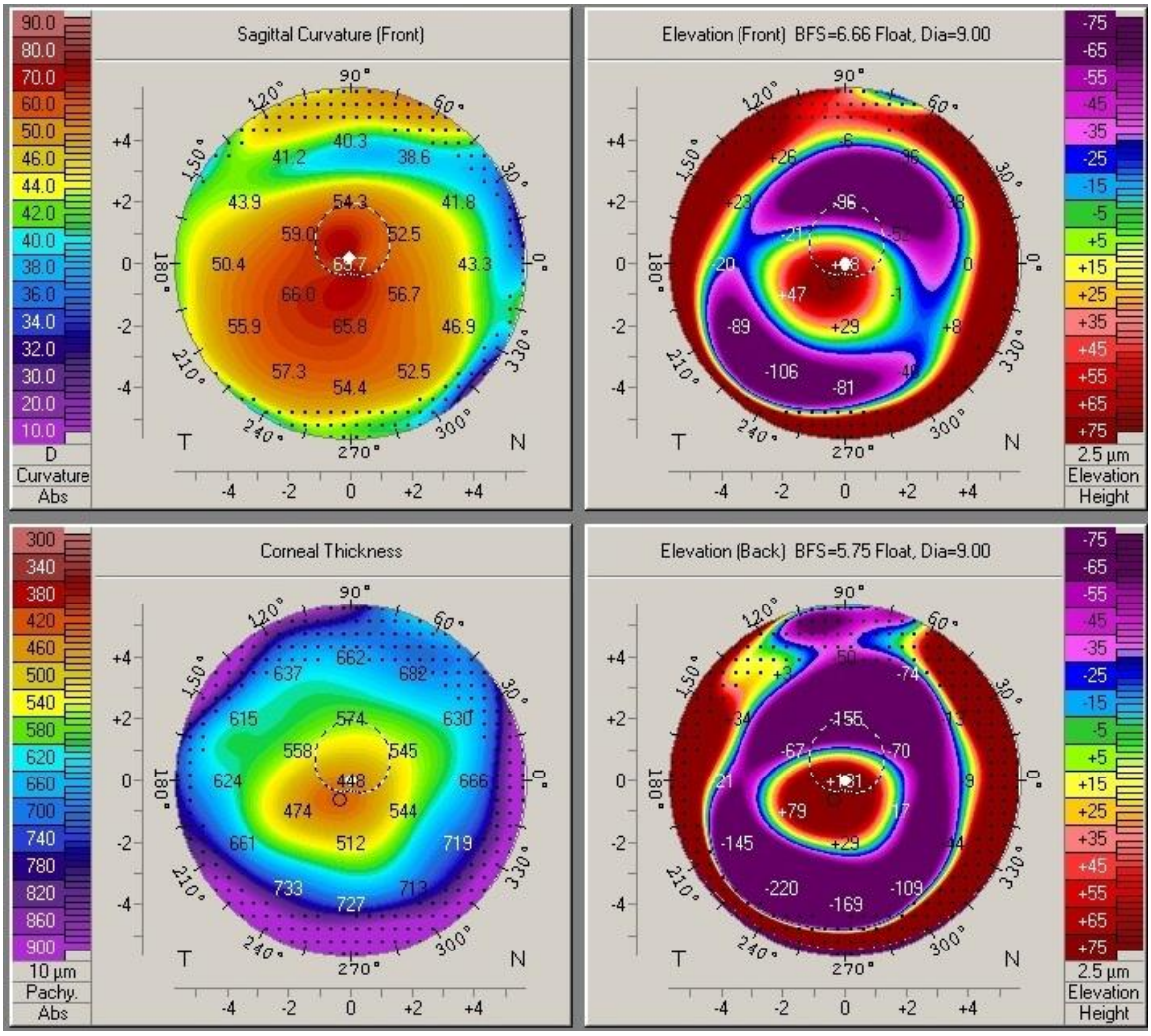

Figure 5: Example of Pentacam readings from a patient with keratoconus. Top left shows the corneal curvature, with inferior steepening. Bottom left shows the corneal thickness, with central thinning. [44]

The Ocular Response Analyzer (Reichert) is a relatively new method for measuring the biomechanical properties of the cornea in vivo, although current metrics show significant overlap between normal and KC corneas, causing question as to the method's precision in distinguishing the two for definitive

diagnosis. Confocal and specular microscopy can be employed to assess changes within the corneal sublayers which often occur with KC, but are not specific to KC. These include irregularity of stromal keratocytes, pleomorphism and polymegathism of endothelial cells, and epithelial cell abnormalities. [46]

Etiology/ Risk Factors

Although development of KC involves complex interactions between environmental and genetic factors, their relative contributions are currently unknown. Recognized environmental influences include contact lens wear and chronic eye rubbing (usually associated with general atopy or a more specific allergic eye disease). Processes such as inflammation, degeneration, and scarring inflict damage to corneal tissue; however, as is the case in many complex diseases, it is extremely challenging to distinguish primary disease mechanisms from secondary effects, or determine which elements are simply associative. Efforts at understanding the pathogenesis of KC are further confounded by the fact that most research has been focused on advanced presentations of the disease, wherein the origins of the observed pathologies are too distant to be traced retrospectively to distinguish individual pathways from one another. The diversity and abundance of factors that can lead to corneal ectasia such as that seen in KC makes it seem unlikely that there exists a single pathway by which the disease manifests, and more likely that the clinical

appearance of KC is a common end of many different pathways, either independently converging or simultaneously compounding. Despite these complications, comparison of normal and KC tissue with regards to protein composition, structure, biomechanics, and genetics, reveals key differences which inform current theories about underlying disease mechanisms and have provided the starting points for development of treatment strategies such as photodynamic CXL.

KC cornea demonstrates a difference in expression of several corneal proteins relative to normal cornea including up-regulation of decorin and keratocan proteoglycans, and differential expression of several enzymes involved in tissue remodeling. [47] Notably, there is a significant reduction in LOX and collagen transcript levels in KC corneal epithelia, and LOX activity isolated from the tear film correlated with disease severity. [48] KC corneas demonstrate alterations in stromal collagen distribution and orientation, also in proportion to the severity of the case. This is consistent with a mechanism of KC progression involving inter-fibrillar or inter-lamellar slippage resulting in redistribution of collagen within the tissue. [49] This mechanism is further supported by the above-discussed observations of reduced lamellar interlacing within the anterior central KC stroma, and fewer lamellar insertions into Bowman's layer. [36] X-ray diffraction studies have shown that the normal orthogonal orientation of deeper stromal lamellae [40] is drastically altered in the apical region of advanced KC, and that the

pattern of redistribution of collagen away from the apical cone is variable between individual cases. [37,49]

Although the majority of KC cases are sporadic, and the hereditary pattern is neither prominent nor predictable, the prevalence of KC in first degree relatives of index cases is significantly higher than that of the general population. [50] There is a high concordance among monozygotic twins, including a high degree of phenotypic similarity. [51] KC has also been associated with a range of hereditary conditions including Down's syndrome, Lever congenital amaurosis, atopy, and Marfan's syndrome. However, the causative genetic variants of these conditions have not been consistently identified in isolated cases of KC. Although many candidate genes have been identified, no contributing gene has yet been found. Regardless, genetic analysis of global scale is beginning to elucidate affected pathways, and genetic susceptibility is agreed upon as a key factor in the pathogenesis of KC. [52]

Reconciling the interplay of genetic and environmental influences in the etiology of KC is still the realm of speculation. However, these findings may help to explain how an environmental insult such as chronic eye rubbing can have such a damaging impact in KC but not normal corneas: a collagen suprastructure which is genetically predisposed to weakness and slippage is made vulnerable to mechanical stress from the environment. This is the so-called "second hit" hypothesis, that genetic factors may make an individual more prone, but

environmental factors are necessary to initiate or accelerate the progression of KC.

Review of Major Treatments Prior to CXL

For decades, the management of KC has been focused on mitigating symptoms, mainly improving vision with corrective lenses. There is no cure, and before collagen cross-linking, there was no way to stop progression, thus corneal transplant was often inevitable. Many of the treatments employed prior to CXL's FDA approval (2016) are still relied upon for patients with mild cases or those who have contraindications which preclude them from CXL treatment. These modalities are effective in improving visual acuity, but they do not prevent it from getting worse as KC progresses. The next section provides a brief background on some of the more commonly employed options.

Contact Lenses

The only non-interventional options are corrective lenses. Spectacles are only effective at correcting regular astigmatism and very low amounts of irregular astigmatism, thus only sufficing in very early cases of KC. Once the cylindrical power (a measure of astigmatism) increases beyond 4.0 diopters, contact lenses become necessary. These are usually rigid gas permeable lenses as opposed to normal soft contact lenses. Rigid lenses can flatten the cone of the KC cornea, giving it a more regular shape, whereas soft lenses tend to conform to the

irregular shape of the KC cornea, thus diminishing their corrective effect. Several varieties of custom contact lenses have been employed, each aimed at accommodating different phenotypes of KC cornea. [53]

Surgery

Interventional options include various types of keratoplasty (corneal surgery) as well as insertion of intracorneal rings (ICRs).

Conductive keratoplasty uses low-energy radiofrequency current to apply heat to the flat axis of the peripheral KC cornea. The heat causes collagen in the peripheral cornea to shrink, which increases the steepness on that access at the central cornea, thereby reducing astigmatism. It is only a temporary fix, as re-steepening usually occurs, and the results are not always predictable due to variable tissue response to thermal treatment. Thus, conductive keratoplasty is not preferred. Penetrating keratoplasty (corneal transplant) is inevitable in the 10-25% of KC patients for whom progression has passed the point of possible visual rehabilitation. Because corneal tissue is avascular, tissue match between donor and host is relatively easy, and risk of complications is relatively low. However, reported complications include allograft rejection, more astigmatism, endothelial cell damage, and the side effects that come with long-term use of topical corticosteroids (a requirement after transplantation). This procedure is indicated for advanced progressive disease with significant corneal scarring. Because rejection episodes are usually endothelial in origin, a recent trend is to remove

only the diseased part of the cornea, sparing the healthy endothelial cells (lamellar keratoplasty). This technique has been shown to have fewer post-operative complications; however, full-thickness penetrating keratoplasty tends to have slightly better outcomes in terms of final best corrected visual acuity (BCVA).

Intracorneal rings are made from polymethylmethacrylate, a biocompatible plastic otherwise known as acrylic. Insertion into the peripheral cornea to increase its thickness to achieve a flattening of the central cornea, as predicted by the Barraquer thickness law: adding material to the peripheral cornea flattens the central cornea whereas removing material from the periphery steepens it. These segments also provide a biomechanical reinforcement for the thin ectatic cornea. The radial positioning of the insert, its diameter and thickness, as well as its distance from the corneal apex are variables by which the desired effect can be achieved. ICRs are contraindicated in immunocompromised patients, or those with habitual eye rubbing. There is no improvement of visual disturbance caused by corneal scarring, and the procedure cannot be performed on corneas of thickness < 350 micrometers at the thinnest location, in which case lamellar keratoplasty would be indicated. This procedure is also more complex, and the traditional mechanical technique of creating the tunnel into which the segment is inserted is very much an art. Minor imperfections or mistakes made by a less-experienced surgeon are usually to blame for undesired outcomes or rare

complications, and advances in corneal tomography and the increasing use of femtosecond lasers for tunnel creation have reduced these. Even if insertion is perfect, patients may be left with aberrations and night glare, although these usually diminish gradually after 6 months for unknown reasons (possibly neural compensation/ plasticity in the visual cortex). There are other treatment modalities for KC including laser surgery, placement of a variety of intraocular lenses, partial or crescent-shaped transplants, and combinations of these. However, the only treatment which can actually halt the progression of KC is riboflavin/UVA-induced corneal collagen cross-linking (CXL). [53]

CXL

Corneal collagen cross-linking (CXL) increases the stiffness and stability of the corneal stroma with the aim of arresting KC progression and avoiding corneal transplant (keratoplasty). This novel approach uses riboflavin as a photosensitizer, excitable by ultraviolet-A (UVA) irradiation, to induce inter-collagen fiber bonding in the otherwise cross-link deficient KC cornea. The general outcome is strengthening, thickening, and flattening of the anterior corneal stroma. Although some cases do show a slight improvement in visual acuity, the major objective is to simply prevent it from getting worse. This is a revolution in the treatment paradigm for KC, especially for young patients, potentially saving them from a lifetime of declining vision, not to mention the cost and complications associated with corneal transplantation.

As discussed previously, collagen molecules are enzymatically cross-linked in a mechanism dependent on post-translational modifications by lysyl oxidase. Lysyl oxidase malfunction is implicated in KC, either due to a gene defect or some other factor causing deficiency or ineffectiveness of the enzyme, thus resulting in fewer cross-links and weak, slippage-prone tissue. Non-enzymatic cross-linking by sugar aldehydes (AGEs) also occurs and increases with age. Cross-links can be induced for therapeutic purposes with chemical agents such as glutaraldehyde or formaldehyde, but these cannot be targeted. On the other hand, the photopolymerization effect of photo-oxidative reactions

induced by a photosensitizer and ionizing radiation can be localized to only the tissue exposed to the radiation. Riboflavin and ultraviolet-A (RFUVA) has emerged as the preferred method for therapeutic photopolymerization because its effect can be localized, riboflavin is nontoxic and bioavailable, a short duration of therapy is sufficient, and the transparency of the cornea is left unaltered. Here, “CXL” will refer specifically to RFUVA.

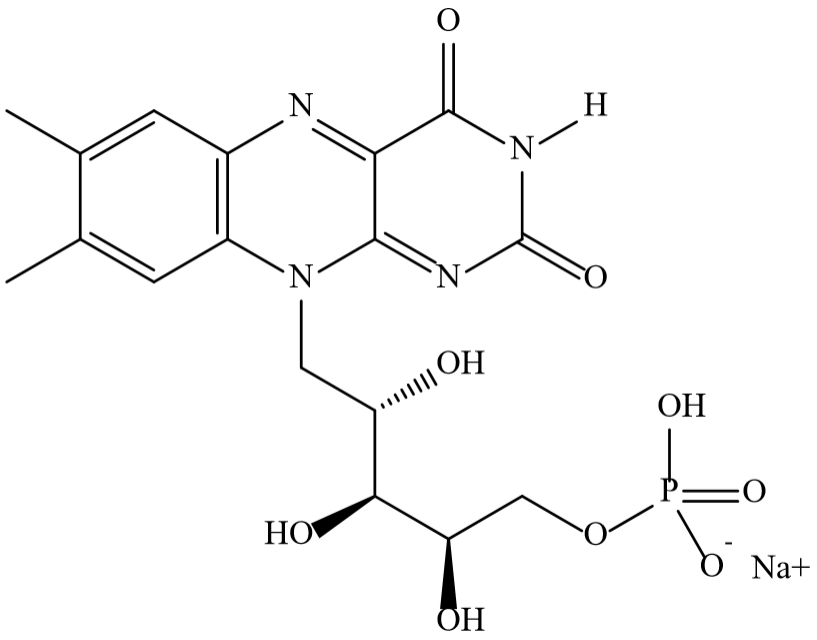

Figure 6: The molecular structure of riboflavin. [54]

The exact mechanisms of the reactions induced by CXL are still being elucidated. Current research suggests that CXL exerts its effect at the molecular level, as opposed to the lamellar level. [55] Riboflavin’s charged nature makes it hydrophilic and thus permeable within the corneal stroma (see Figure 6 above).

Cross-links form between collagen molecules (involving AGEs), [56] between proteoglycan core proteins, and between PG core proteins and collagens. [57] It is the carbonyl groups rather than amine groups of the proteins that participate, and singlet oxygen plays a major role. [58]

Energetically, CXL is comparable to photosynthesis – radiation energy is transformed into chemical energy with the aid of a pigment. The transfer of energy into chemical bonds means that very little heat is produced. In CXL, there is a maximum temperature increase of 2-3 °C, an amount not sufficient to cause the observed changes, nor to cause tissue damage. [59] Instead, riboflavin molecules absorb light energy and move from a ground state to an electronically excited state (singlet riboflavin).

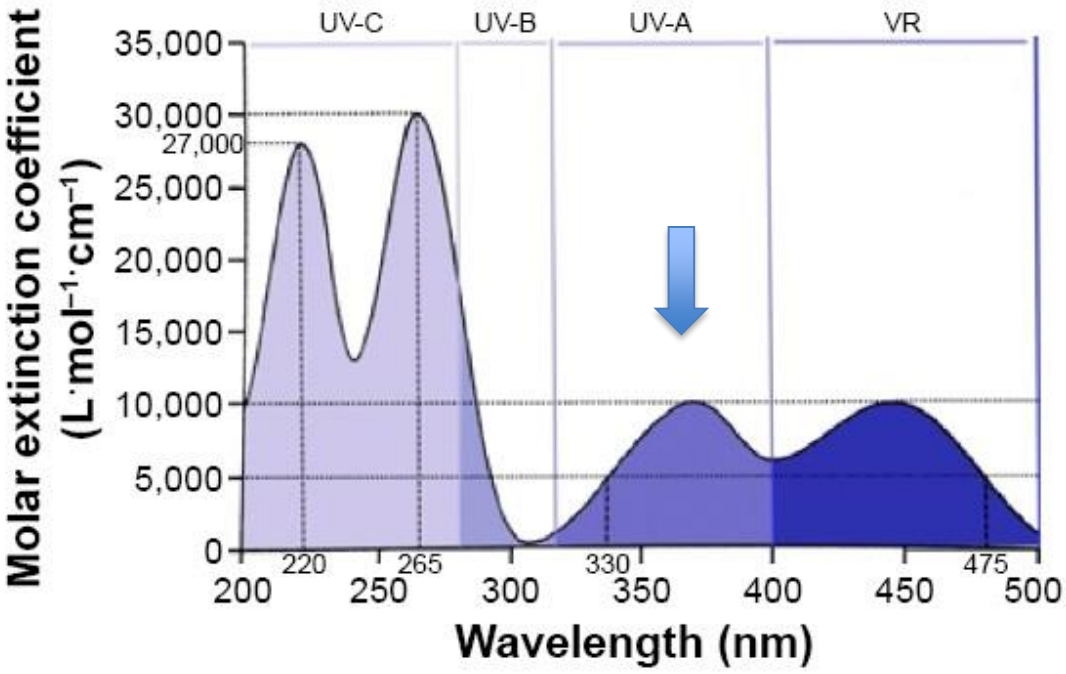

Figure 7: Riboflavin's absorption spectrum. [60]

Riboflavin's absorption spectrum dictates the wavelength(s) of light at which it absorbs the most energy. As shown by Figure 7, this spectrum has a peak that matches the wavelength of ultraviolet-A (365 nm), thus making riboflavin/UVA an effective pair for photoexcitation. Excited singlet riboflavin rapidly converts to triplet riboflavin, which then participates in one of two reaction processes. In the type II process, triplet riboflavin interacts with oxygen to create singlet oxygen radicals which then oxidize the carbonyl groups of amino acids in collagen (especially histidine), to create covalent linkages. However, if oxygen is depleted by UVA, the type I process dominates, whereby excited riboflavin triplets react directly with their substrates in collagen via hydrogen or electron

transfer reactions. [61] Thus photo-oxidation of susceptible amino acids is the primary process, with subsequent covalent cross-linking occurring via secondary, light-independent reactions. Figure 8 provides a conceptual flowchart for the interactions of substrate and riboflavin in the primary processes (Type I and Type II).

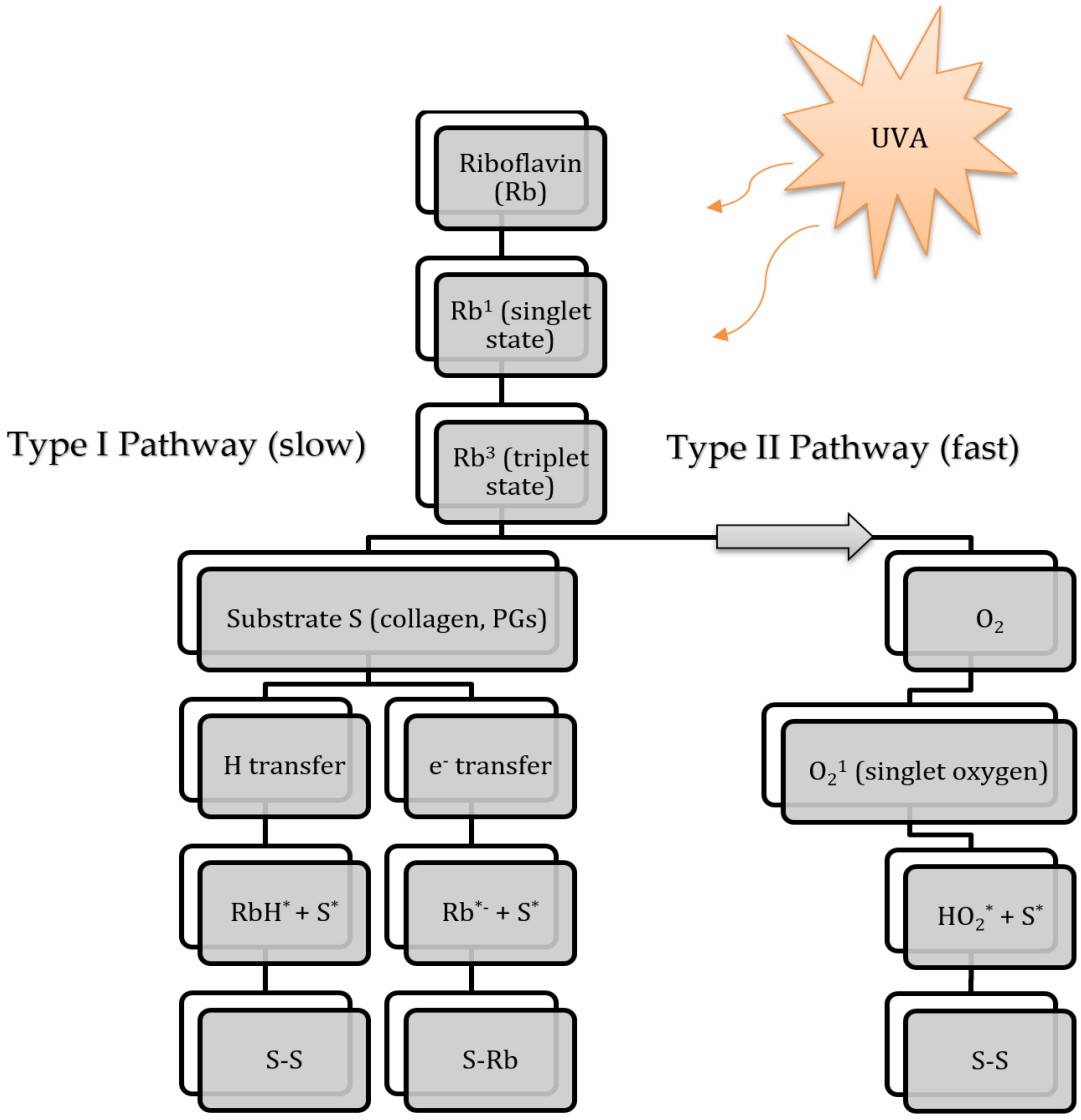

Figure 8: Photochemical reaction pathways of RFUVA CXL. [61–63]

There are five photo-oxidizable amino acids with varying reactivity to singlet oxygen and varying abundance in corneal collagen: tryptophan, tyrosine, cysteine, methionine, and histidine. While cysteine and tryptophan are highly reactive, they are nearly nonexistent in corneal collagen. Methionine, despite being oxidizable, is not known to participate in the formation of cross-links. Tyrosine can participate in cross-linking by a type I process but is therefore inhibited by the presence of oxygen which favors the type II pathway. [64,65] Thus, histidine appears to be the major amino acid player in protein-protein CXL reactions. This is supported by the finding that proteins lacking histidine do not form cross-links in the presence of singlet oxygen. [66]

Effects

With current technology, RFUVA-induced cross-links in the cornea cannot be visualized with labeling methods or microscopic techniques. However, there are measurable changes in certain properties of the tissue which can be used as indirect indication of cross-linking having occurred, and to what extent. Note, most of these studies have been conducted on ex vivo non-human corneas, but the difference in tissue between species in terms of composition and organization is negligible. Stress-strain experiments indicate that cross-linked tissue is stiffer and less elastic, and that this firming effect is sufficient to compensate for the decreased stability seen in KC. [67–69] There is also a decrease in the tissue's tendency to swell, [70] and a 4.5% increase in the diameter of collagen fibers in the

anterior stroma. [71] Recent studies have shown a significant increase of proteolytic enzymes in the tear films of KC patients (e.g. MMP), likely contributing to the degradative progression of the disease. [72] However, CXL increases the cornea's resistance to enzymatic degradation, making it less susceptible to thinning but also lengthening the collagen turnover time. [73] Finally, gel electrophoresis reveals the creation of molecular aggregates of greater molecular weight. These varied in size, and included an especially stable polymer not found in normal cornea. [74] This supports the findings that CXL induces several different types of cross-links between numerous substrate pairs, as opposed to one specific type by a single mechanism.

CXL does not exert its effect uniformly through the entire thickness of the cornea, but only where the riboflavin/UVA interaction takes place. The concentration of riboflavin decreases linearly with increased stromal depth, according to its diffusion gradient. [75] Additionally, the intensity of UVA irradiation decreases exponentially with depth, in proportion to the concentration of the attenuating riboflavin (Beer-Lambert law). [76] Thus, there is a much greater interaction of these two components nearer to the corneal surface. In fact, 65% of the light energy is absorbed (and directed into the formation of cross-links) in the first 200 μm of anterior stroma. [68,73] This Beer-Lambert effect has important ramifications for treatment optimization, to be discussed later.

The relevant clinical effects of CXL are focused on halting disease progression as measured by four major criteria pre- and post-operation: topography, visual acuity, refraction/ astigmatism, and central corneal thickness. A meta-analysis of 49 human studies demonstrates statistically significant improvements in all outcomes at 1 year post-operation. Maximum keratometry values (a topographic measure of corneal steepness) were reduced by about 1 diopter. Best corrected visual acuity (BCVA) improved somewhat, although uncorrected acuity showed no improvement. Improvements in astigmatism were an average change of -0.7 diopters at 1 year, and -0.5 diopters at 24 months. Finally, there was a reported average reduction of -14.4 μm in central corneal thickness. [77]

Cellular changes following CXL have been considered. The removed epithelium is restored in 4 days following treatment, and no damage to limbal stem cells, nor abnormalities in cell proliferation. Within the stroma, wound healing mechanisms are triggered, including keratocyte apoptosis. 3-6 months after CXL, new keratocytes migrate from the periphery to the center concurrent with an increased density of the ECM in the anterior stroma. The difference in density creates a difference in reflectivity upon confocal microscopy termed the “late demarcation line,” providing a useful clinical tool for confirming CXL impact. [78] These structural changes, coupled with the synthesis of new collagen by migrating keratocytes, further support the long-term stability of CXL’s effect on corneal biomechanics. Finally, endothelial cell changes show no significant

difference between CXL and untreated eyes. This is because 90% of the UVA energy is absorbed in the riboflavin-treated cornea (approximately 400 μm thick). Thus, the amount of radiation reaching the endothelial layer is about half (0.18 mW/cm^2)[79] the minimum amount needed to cause cellular damage (0.35 mW/cm^2). [80]

Analysis of 24 CXL patients 10 years post-operatively confirms long-term efficacy in stabilizing KC corneas, finding significant improvement in BCVA and corneal topography measures. Furthermore, although damage to the endothelium has historically been the major safety concern in CXL, this analysis found no decline in endothelial cell count beyond what would be expected with normal aging in untreated eyes. [81]

Current Standard Procedure: Avedro's KXL System

Following the promising results of initial experiments using photosensitizer to generate cross-links in the eye, [82] CXL was first implemented for the treatment of keratoconus in 1998. The pilot study, conducted in Dresden, halted progression in all 22 patients and had no immediate side effects, [67] paving the way for the current clinical treatment which finally gained FDA approval in April of 2016.

The original “Dresden protocol” involved removal of the central 7 mm of corneal epithelium followed by administration of 0.1% riboflavin in 20% dextrin solution for 5 minutes before, and every 5 minutes during, a 30-minute irradiation period with 370 nm wavelength UVA at 3.0 mW/cm^2 intensity. The differences between this and the current treatment protocol are as follows: Avedro’s Photrexa Viscous riboflavin solution has a concentration of 0.146% riboflavin (also in 20% dextrin). Photrexa Viscous is applied every 2 minutes for 30 minutes before, and every 2 minutes during, the 30-minute irradiation period. Before beginning irradiation, thorough absorption of riboflavin through the entire depth of the cornea is confirmed by presence of flare in the anterior chamber upon slit-lamp examination (Tyndall effect). Because Photrexa Viscous is hypertonic, it draws water out of the cornea, reducing its thickness. If the cornea is measured to be less than 400 μm thick (by ultrasound pachymetry) after the initial “soak” period, 1-2 drops of a different solution (Photrexa) are applied every 5-10 seconds to swell the cornea back to above threshold. Photrexa has the same concentration of riboflavin, but without the dextrin, making it hypotonic. A minimum corneal thickness of 400 μm is required to ensure that the energy reaching the endothelium is below the damage threshold.

The FDA lists no contraindications. The most common ocular adverse reactions observed during clinical trials were corneal opacity (haze), punctate keratitis, corneal striae, corneal epithelium defect, eye pain, and reduced visual

acuity (blurry vision). The majority of adverse events resolved during the first month; however, patients are counseled that vision can take up to 1 year to fully stabilize. [54]

MAJOR PROPOSED PROCEDURAL MODIFICATIONS

Broadly speaking, the major parameters that can be modified are how the light energy is delivered (and how much), and the composition of the riboflavin-containing solution and how it is delivered. The major goal of treatment optimization is to minimize the total treatment time, while maximizing clinical effect and patient comfort. Shorter treatments are more comfortable for the patient, allow a higher throughput for the practitioner, and present a theoretically lower risk of infection.

Irradiance

According to the Bunsen-Roscoe law, all photochemical reaction mechanisms depend only on the total absorbed energy and are statistically independent of the two factors that determine total absorbed energy – the radiant intensity, and exposure time. [83] This would predict that the extent of photooxidative cross-linking that occurs with CXL will be the same given that the total energy delivered is the same. However, it is known that many photochemical reactions (e.g. film photography) demonstrate Bunsen-Roscoe validity only within a certain range, and it is not yet known how large this range is for RFUVA CXL. This led to exploration of the equivalence of various increased light intensities and proportionally decreased irradiation durations in regards to efficacy.

Stress-strain experiments on porcine corneas have shown equivalence in stiffening effect between standard CXL (S-CXL) and an accelerated CXL (A-CXL) using 10 mW/cm^2 for 9 minutes. [84] Follow up experiments saw an equivalent stiffness increase with increasing intensities (and corresponding decreased durations), but only up to approximately 45 mW/cm^2, beyond which there was a sudden drop to no significant difference from controls. [85] Neither study addressed the safety of higher intensities for humans. Shetty et al recently compared 4 patient groups with equivalent total delivered energy: 3 mW/cm^2 for 30 minutes (Group 1, S-CXL), 9 mW/cm^2 for 10 minutes (Group 2), 18 mW/cm^2 for 5 minutes (Group 3), and 33 mW/cm^2 for 3 minutes (Group 4). Across the four groups, the clinical CXL effect declined in proportion to the increase in intensity. While groups 1 and 2 showed the typical flattening effect evidenced by reduced keratometry values, groups 3 and 4 showed stabilization but not reduction. Furthermore, demarcation lines, which denote the area of keratocyte apoptosis caused by RF penetration and thus provide an indirect measure of CXL effect, were less and less defined with increasing intensities. Disease progression was observed only in groups 3 and 4. [86] Furthermore, although this study found no significant difference in endothelial cell count, other research has indicated transient changes in cell density and morphology following A-CXL at 18 mW/cm^2 for 5 minutes. [87] While the endothelial cells do recover safely after an average of 6 months, this is clear evidence of endothelial effects following A-CXL, the repercussions of which need further exploration.

The apparent failure of the Bunsen-Roscoe law in the case of A-CXL is likely because the treatment effect is not achieved by a single photochemical reaction but by multiple different pathways and likely including other downstream effects due to long term cellular changes which have yet to be elucidated. One explanation is that higher intensity radiation induces faster consumption of oxygen and therefore reduces the efficiency of the oxygen-dependent (type II) reactions. The importance of oxygen availability is demonstrated by data showing a complete lack of CXL effects when performed in anaerobic conditions. [61]

Because photochemically generated reactive oxygen species (ROS) are needed to react with proteoglycan core proteins and collagen to induce cross-linking, more protein oxidation should result in more cross-linking. Thus, the power of different CXL modalities can be assessed by quantifying advanced oxidation protein products (AOPPs), a measure of protein oxidation. One method of increasing oxygen availability during CXL is to use pulses of light as opposed to a continuous exposure. Theoretically, pulsed light accelerated CXL (PLA-CXL) allows stromal oxygen concentrations to be replenished, enabling delivery of an equivalent dose of energy in less time without sacrificing photochemical efficiency, thus side-stepping the disadvantage of continuous exposure A-CXL. Supportive of this theory, recent research measured more AOPPs after PLA-CXL than both S-CXL and A-CXL. [88] Although it is assumed that higher levels of

AOPPs will result in greater cross-linking, further studies directly equating AOPP levels with clinical effect are needed for confirmation.

Modeling

Mathematical models, scaled to experimental results, have been formulated to predict the extent and distribution of stromal stiffness increase as a function of variable treatment parameters (riboflavin concentration, radiation intensity, time). Fick's second law of diffusion, the Lambert-Beer law of light absorption, and reaction rate equations are used to predict the rate of cross-linking (polymerization rate). Experimental results for stiffness increase are correlated with the simulated polymerization rate increase. [62,63] Recall that riboflavin absorbs UVA and induces polymerization, and its concentration decays linearly as a function of corneal depth. Meanwhile, the intensity of light decays exponentially with depth. This is important for predicting not just the total stiffness change of the cornea (as has been measured in efficacy experiments to date), but also the distribution of that change across its depth. A reduction in riboflavin concentration results in deeper light penetrance and a more uniform effect. Conversely, increasing the concentration results in more energy being absorbed nearer to the corneal surface but declining more precipitously as you move deeper, creating a much less uniform effect profile. This is supported by data showing shallower demarcation lines with A-CXL (although reports of exact depth vary widely between 100-150 um [89] and 294 um [90]) as opposed to ~300 um in S-

CXL. [78] This appears to be a function of total treatment time rather than radiation intensity given that pulsed exposures achieve greater demarcation line depths at the same intensity. [91] Furthermore, the less uniform the profile, the lower the total stiffness increase. One interesting modeled prediction is that, with riboflavin concentration held constant at 0.1%, the polymerization rate increases with increasing intensities but then saturates at approximately 3.0 mW/cm^2. Therefore, although the total amount of cross-linking may vary as a function of time, the actual rate at which it happens does not get any faster with excessively high intensities. This simulation corroborates quite well with the experimental data discussed above. Furthermore, it validates the parameters of S-CXL for best effect within the constant exposure modality. In fact, this model [62] predicts the slightly higher RF concentration of 0.146% for optimal polymerization rate while keeping the light penetrance below the endothelial damage threshold.

Riboflavin Delivery

Other experimental treatment modalities attempt to achieve the same clinical effect as S-CXL without removing the epithelium. This reduces post-operative pain, [92] and allows for faster return to optimal vision. Unfortunately, riboflavin diffusion into the stroma is dramatically hindered by the intact epithelium, showing a detectable penetration depth of only 20 μm compared to 400-600 μm when the epithelium is removed. [75] Therefore, various methods have

been employed to try to increase RF penetrance without damaging the epithelium.

The use of the chemical agent benzalkonium chloride or EDTA to reduce epithelial resistance has demonstrated safety but increased corneal stiffness by an amount only 1/5th that of S-CXL with epithelial debridement, [93,94] and anywhere from 23% [95] to 55% [96] of patients showed continued disease progression. One study using a combination of chemical enhancers (gentamicin 0.3%, EDTA 0.01%, and benzalkonium chloride 0.01%) successfully stabilized corneal curvature, but still demonstrated a less-pronounced effect than S-CXL. [97] Because riboflavin is a charged molecule of small molecular weight, it is a good candidate for iontophoresis. Use of iontophoresis with 0.1% hypotonic riboflavin and double-enhancement with EDTA and trometamol under accelerated irradiation of 10 mW/cm^2 for 9 minutes did prevent KC progression up to 1 year without endothelial cell count change or reduction in central corneal thickness. However, no demarcation line was observed, and the biomechanical effect, although greater than typical trans-epithelial modalities, was still inferior to S-CXL. [98] Some encouraging results were obtained very recently using Vitamin E as an enhancer. Disease progression was halted and there was no detectable endothelial damage up to 2 years post-operatively. However, only 19 patients were studied and a control group to provide comparison to S-CXL was not employed. [99]

CONCLUDING REMARKS

There are a few things to keep in mind which the current literature does not extensively address.

Regarding the effectiveness of various CXL modalities in compensating astigmatism, it is true that a general flattening of the cornea tends to improve refractions and reduce astigmatism; however, refractions depend on subjective patient responses and are notoriously difficult and variable in KC patients due to the multifocal optics of the distorted cornea. Thus, reference to improved refractive outcomes are insufficient on their own to indicate treatment efficacy.

Current assessment of endothelial safety focuses on the endothelial cells themselves (density, morphology), but evidence is lacking regarding the impact of higher UV intensities on the nerves of the endothelial layer (the subbasal plexus). If nerve damage here would negatively impact the health of the endothelium, the status of the subbasal plexus should be included in assessments of safety.

The delivery of riboflavin solution by the typical drop method introduces complications. Because drops disperse upon the eye, the effective concentration at the ocular surface is significantly less than the initial concentration of the solution. The placement of a Landers vitrectomy silicone ring on the limbus [63,95]

to maintain a pool of solution over the treatment area will result in more consistent penetrance and concentrations within the stroma. Also, the shielding effect caused by excess riboflavin at the ocular surface makes actual light penetrance (and therefore energy delivery) both lower than expected and also variable, depending on the changing thickness of this layer between drops. Washing the riboflavin film before irradiation would make treatments more consistent/ reproducible, and should also reduce the intensity requirement. However, without constant reapplication during irradiation, intrastromal riboflavin concentrations will fall, potentially exposing the endothelium to too much radiation. The temporal component introduced by this diffusion-dependent intrastromal de-shielding would need further exploration.

Finally, theoretical models are useful but are not yet comprehensive. For example, current models only account for the energy delivered to the reaction system via light absorbance, without consideration of light scatter. Furthermore, more depth-dependent analyses of CXL effect are needed to precisely model the uniformity and distribution of cross-linking.

Summary

KXL is an effective and safe treatment for KC. Although the exact mechanisms are still not fully understood, there appear to be certain requirements and limitations for any RFUVA-type CXL paradigm: oxygen

availability is an important factor, the Bunsen-Roscoe law does not neatly apply to CXL reactions, epithelium removal is still superior to trans-epithelial modalities (although some of the methods for facilitating stromal riboflavin delivery may prove helpful for shortening the pre-soak period), and the optimal constant-exposure irradiation is likely no greater than 18 mW/cm^2 intensity for a period of 5 minutes (maintaining the total energy delivered at 5.4 J/cm^2), although PLA-CXL may prove to have a different optimum.

With a complete understanding of various treatment parameters' specific impact on outcomes, and therefore more precise models, it seems likely that physicians will soon be able to tailor each treatment to be specific to the individual's unique disease profile (severity, phenotypic presentation, corneal thickness, etc.). In the meantime, the established requirements and limitations for producing clinically effective CXL should inform research focus. By current understanding, PLA-CXL, at intensities up to 18 mw/cm^2, seems to have the greatest potential for decreasing treatment times while maintaining optimal clinical effect.

REFERENCES

1. Kivelä, T., Messmer, E. M. & Rymgayłło-Jankowska, B. in *Eye Pathology* (eds. Heegaard, S. & Grossniklaus, H.) 79–154 (Springer Berlin Heidelberg, 2015). doi:10.1007/978-3-662-43382-9_3
2. in *Common Eye Diseases and their Management* (eds. Galloway, N. R., Amoaku, W. M. K., Galloway, P. H. & Browning, A. C.) 7–15 (Springer London, 2006).
3. CRNEADGM.JPG (JPEG Image, 307 × 497 pixels). Available at: http://www.doctorc.net/EYE/CRNEADGM.JPG. (Accessed: 12th February 2017)
4. Alberto, D. & Garello, R. Corneal Sublayers Thickness Estimation Obtained by High-Resolution FD-OCT. *International Journal of Biomedical Imaging* **2013,** 989624 (2013).
5. Hanna, C., Bicknell, D. S. & O'brien, J. E. Cell turnover in the adult human eye. *Archives of Ophthalmology* **65,** 695–698 (1961).
6. Wang, L., Deng, S. X. & Lu, L. Role of CTCF in EGF-induced migration of immortalized human corneal epithelial cells. *Investigative Ophthalmology and Visual Science* **53,** 946–951 (2012).
7. Li, W., Hayashida, Y., Chen, Y.-T. & Tseng, S. C. G. Niche regulation of corneal epithelial stem cells at the limbus. *Cell Research* **17,** 26–36 (2007).

8. Matsuda, M., Ubels, J. L. & Edelhauser, H. F. A larger corneal epithelial wound closes at a faster rate. *Investigative Ophthalmology and Visual Science* **26,** 897–900 (1985).
9. DelMonte, D. W. & Kim, T. Anatomy and physiology of the cornea. *Journal of Cataract & Refractive Surgery* **37,** 588–598 (2011).
10. Meek, K. M. & Boote, C. The use of X-ray scattering techniques to quantify the orientation and distribution of collagen in the corneal stroma. *Progress in Retinal and Eye Research* **28,** 369–392 (2009).
11. Winkler, M. *et al.* Three-dimensional distribution of transverse collagen fibers in the anterior human corneal stroma. *Investigative Ophthalmology and Visual Science* **54,** 7293–7301 (2013).
12. Tamura, Y., Konomi, H., Sawada, H., Takashima, S. & Nakajima, A. Tissue distribution of type VIII collagen in human adult and fetal eyes. *Investigative Ophthalmology and Visual Science* **32,** 2636–2644 (1991).
13. Mienaltowski, M. J. & Birk, D. E. in *Progress in Heritable Soft Connective Tissue Diseases* (ed. Halper, J.) **802,** 5–29 (Springer Netherlands, 2014).
14. Baldock, C. *et al.* Three-dimensional reconstructions of extracellular matrix polymers using automated electron tomography. *Journal of Structural Biology* **138,** 130–136 (2002).
15. Yamamoto, S. *et al.* The subfibrillar arrangement of corneal and scleral collagen fibrils as revealed by scanning electron and atomic force microscopy. *Archives of Histology and Cytology* **63,** 127–135 (2000).

16. Julianna Skinner :: SlidePlayer. Available at: http://slideplayer.com/user/5342526/. (Accessed: 12th February 2017)
17. Yamauchi, M., Chandler, G. S., Tanzawa, H. & Katz, E. P. Cross-Linking and the Molecular Packing of Corneal Collagen. *Biochemical and Biophysical Research Communications* **219,** 311–315 (1996).
18. Robins, S. P. Biochemistry and functional significance of collagen cross-linking. *Biochemical Society Transactions* **35,** 849–852 (2007).
19. Brüel, A., Ortoft, G. & Oxlund, H. Inhibition of cross-links in collagen is associated with reduced stiffness of the aorta in young rats. *Atherosclerosis* **140,** 135–145 (1998).
20. File:Tropocollagen cross-linkage lysyl oxidase (EN).svg. *Wikipedia*
21. Robins, S. P., Shimokomaki, M. & Bailey, A. J. The chemistry of the collagen cross-links. Age-related changes in the reducible components of intact bovine collagen fibres. *The Biochemical Journal* **131,** 771–780 (1973).
22. Yamauchi, M., London, R. E., Guenat, C., Hashimoto, F. & Mechanic, G. L. Structure and formation of a stable histidine-based trifunctional cross-link in skin collagen. *The Journal of Biological Chemistry.* **262,** 11428–11434 (1987).
23. Robert, L., Robert, A.-M. & Labat-Robert, J. The Maillard reaction--illicite (bio)chemistry in tissues and food. *Pathologie-biologie* **59,** 321–328 (2011).
24. Robins, S. P. *et al.* Increased skin collagen extractability and proportions of collagen type III are not normalized after 6 months healing of human

excisional wounds. *Journal of Investigative Dermatology* **121,** 267–272 (2003).

25. Michelacci, Y. M. Collagens and proteoglycans of the corneal extracellular matrix. *Brazilian Journal of Medical and Biological Research* **36,** 1037–1046 (2003).
26. Massoudi, D., Malecaze, F. & Galiacy, S. D. Collagens and proteoglycans of the cornea: importance in transparency and visual disorders. *Cell and Tissue Research* **363,** 337–349 (2016).
27. Meek, K. M. & Knupp, C. Corneal structure and transparency. *Progress in Retinal and Eye Research* **49,** 1–16 (2015).
28. Galiacy, S. D. *et al.* Matrix metalloproteinase 14 overexpression reduces corneal scarring. *Gene Therapy* **18,** 462–468 (2011).
29. Chen, S., Mienaltowski, M. J. & Birk, D. E. Regulation of corneal stroma extracellular matrix assembly. *Experimental Eye Research* **133,** 69–80 (2015).
30. Sun, M. *et al.* Collagen V is a dominant regulator of collagen fibrillogenesis: dysfunctional regulation of structure and function in a corneal-stroma-specific Col5a1-null mouse model. *Journal of Cell Science.* **124,** 4096–4105 (2011).
31. Scott, J. E. Proteoglycan-fibrillar collagen interactions. *Biochemical Journal* **252,** 313–323 (1988).
32. Berman, E. R. *Biochemistry of the Eye*. (Springer Science & Business Media, 2013).

33. Sherratt, M. J., Holmes, D. F., Shuttleworth, C. A. & Kielty, C. M. Substrate-dependent morphology of supramolecular assemblies: fibrillin and type-VI collagen microfibrils. *Biophysical Journal* **86,** 3211–3222 (2004).
34. Beecher, N. *et al.* Collagen VI, conformation of A-domain arrays and microfibril architecture. *The Journal of Biological Chemistry* **286,** 40266–40275 (2011).
35. Wiberg, C., Heinegård, D., Wenglén, C., Timpl, R. & Mörgelin, M. Biglycan organizes collagen VI into hexagonal-like networks resembling tissue structures. *The Journal of Biological Chemistry* **277,** 49120–49126 (2002).
36. Morishige, N. *et al.* Second-harmonic imaging microscopy of normal human and keratoconus cornea. *Investigative Ophthalmology and Visual Science* **48,** 1087–1094 (2007).
37. Meek, K. M. *et al.* Changes in collagen orientation and distribution in keratoconus corneas. *Investigative Ophthalmology and Visual Science* **46,** 1948–1956 (2005).
38. Bergmanson, J. P. G., Horne, J., Doughty, M. J., Garcia, M. & Gondo, M. Assessment of the number of lamellae in the central region of the normal human corneal stroma at the resolution of the transmission electron microscope. *Eye Contact Lens* **31,** 281–287 (2005).
39. Müller, L. J., Pels, E., Schurmans, L. R. H. M. & Vrensen, G. F. J. M. A new three-dimensional model of the organization of proteoglycans and collagen

fibrils in the human corneal stroma. *Experimental Eye Research* **78,** 493–501 (2004).

40. Abahussin, M. *et al.* 3D collagen orientation study of the human cornea using X-ray diffraction and femtosecond laser technology. *Investigative Ophthalmology and Visual Science* **50,** 5159–5164 (2009).
41. Ocular Tissues Biomechanics. *Nguyen Lab* Available at: https://engineering.jhu.edu/tnguy108/research/biomechanics-human-sclera/. (Accessed: 12th February 2017)
42. Boyce, B. L., Grazier, J. M., Jones, R. E. & Nguyen, T. D. Full-field deformation of bovine cornea under constrained inflation conditions. *Biomaterials* **29,** 3896–3904 (2008).
43. Winkler, M. *et al.* Nonlinear optical macroscopic assessment of 3-D corneal collagen organization and axial biomechanics. *Investigative Ophthalmology and Visual Science* **52,** 8818–8827 (2011).
44. Keratoconus - EyeWiki. Available at: http://eyewiki.aao.org/Keratoconus. (Accessed: 4th February 2017)
45. Sinjab, M. M. in *Quick Guide to the Management of Keratoconus: A Systematic Step-by-Step Approach* (ed. Sinjab, M.) 13–58 (Springer Berlin Heidelberg, 2012).
46. Sinjab, M. M. in *Quick Guide to the Management of Keratoconus: A Systematic Step-by-Step Approach* (ed. Sinjab, M.) 1–11 (Springer Berlin Heidelberg, 2012).

47. Joseph, R., Srivastava, O. P. & Pfister, R. R. Differential epithelial and stromal protein profiles in keratoconus and normal human corneas. *Experimental Eye Research* **92,** 282–298 (2011).
48. Shetty, R. *et al.* Attenuation of lysyl oxidase and collagen gene expression in keratoconus patient corneal epithelium corresponds to disease severity. *Molecular Vision* **21,** 12–25 (2015).
49. Hayes, S., Boote, C., Tuft, S. J., Quantock, A. J. & Meek, K. M. A study of corneal thickness, shape and collagen organisation in keratoconus using videokeratography and X-ray scattering techniques. *Experimental Eye Research* **84,** 423–434 (2007).
50. Wang, Y., Rabinowitz, Y. s., Rotter, J. i. & Yang, H. Genetic epidemiological study of keratoconus: Evidence for major gene determination. *American Journal of Medical Genetics* **93,** 403–409 (2000).
51. Tuft, S. J. *et al.* Keratoconus in 18 pairs of twins. *Acta Ophthalmologica* **90,** e482–e486 (2012).
52. Fournié, P., Galiacy, S. D. & Malecaze, F. in *Keratoconus* (ed. Alió, J. L.) 7–12 (Springer International Publishing, 2017). doi:10.1007/978-3-319-43881-8_2
53. Sinjab, M. M. in *Quick Guide to the Management of Keratoconus: A Systematic Step-by-Step Approach* (ed. Sinjab, M.) 59–93 (Springer Berlin Heidelberg, 2012).

54. Drugs@FDA: FDA Approved Drug Products. Available at: http://www.accessdata.fda.gov/scripts/cder/daf/index.cfm?event=overview.process&ApplNo=203324. (Accessed: 9th February 2017)
55. Labate, C., De Santo, M. P., Lombardo, G. & Lombardo, M. Understanding of the viscoelastic response of the human corneal stroma induced by riboflavin/UV-a cross-linking at the nano level. *Publc Library of Science* **10,** e0122868 (2015).
56. Brummer, G., Littlechild, S., McCall, S., Zhang, Y. & Conrad, G. W. The role of nonenzymatic glycation and carbonyls in collagen cross-linking for the treatment of keratoconus. *Investigative Ophthalmology and Visual Science.* **52,** 6363–6369 (2011).
57. Zhang, Y., Conrad, A. H. & Conrad, G. W. Effects of ultraviolet-A and riboflavin on the interaction of collagen and proteoglycans during corneal cross-linking. *Journal of Biological Chemistry* **286,** 13011–13022 (2011).
58. McCall, A. S. *et al.* Mechanisms of corneal tissue cross-linking in response to treatment with topical riboflavin and long-wavelength ultraviolet radiation (UVA). *Investigative Ophthalmology and Visual Science* **51,** 129–138 (2010).
59. Mencucci, R. *et al.* Riboflavin and ultraviolet A collagen crosslinking: in vivo thermographic analysis of the corneal surface. *Journal of Cataract and Refractive Surgery* **33,** 1005–1008 (2007).
60. Kornilovskiy, I. M., Kasimov, E. M., Sultanova, A. I. & Burtsev, A. A. Laser-induced corneal cross-linking upon photorefractive ablation with riboflavin.

Clinical Ophthalmology (2016). Available at: https://www.dovepress.com/laser-induced-corneal-cross-linking-upon-photorefractive-ablation-with-peer-reviewed-fulltext-article-OPTH. (Accessed: 21st February 2017)

61. Kamaev, P., Friedman, M. D., Sherr, E. & Muller, D. Photochemical Kinetics of Corneal Cross-Linking with RiboflavinKinetics of Corneal Cross-Linking. *Investigative Ophthalmology and Visual Science* **53,** 2360–2367 (2012).
62. Huynh, J. Factors Governing Photodynamic Cross-linking of Ocular Coat. (California Institute of Technology, 2011).
63. Schumacher, S., Mrochen, M., Wernli, J., Bueeler, M. & Seiler, T. Optimization Model for UV-Riboflavin Corneal Cross-linking. *Investigative Ophthalmology and Visual Science* **53,** 762–769 (2012).
64. Eastoe, J. E. The amino acid composition of mammalian collagen and gelatin. *The Biochemical Journal* **61,** 589–600 (1955).
65. Michaeli, A. & Feitelson, J. Reactivity of singlet oxygen toward amino acids and peptides. *Photochemistry and Photobiology* **59,** 284–289 (1994).
66. Shen, H. R., Spikes, J. D., Kopecková, P. & Kopecek, J. Photodynamic crosslinking of proteins. II. Photocrosslinking of a model protein-ribonuclease A. *Journal of Photochemistry and Photobiology. B, Biology* **35,** 213–219 (1996).

67. Wollensak, G., Spoerl, E. & Seiler, T. Riboflavin/ultraviolet-a-induced collagen crosslinking for the treatment of keratoconus. *American Journal of Ophthalmology* **135,** 620–627 (2003).
68. Kohlhaas, M. *et al.* Biomechanical evidence of the distribution of cross-links in corneas treated with riboflavin and ultraviolet A light. *Journal of Cataract and Refractive Surgery* **32,** 279–283 (2006).
69. Viswanathan, D., Kumar, N. L., Males, J. J. & Graham, S. L. Relationship of Structural Characteristics to Biomechanical Profile in Normal, Keratoconic, and Crosslinked Eyes. *Cornea* **34,** 791–796 (2015).
70. Wollensak, G., Aurich, H., Pham, D.-T. & Wirbelauer, C. Hydration behavior of porcine cornea crosslinked with riboflavin and ultraviolet A. *Journal of Cataract and Refractive Surgery* **33,** 516–521 (2007).
71. Wollensak, G., Wilsch, M., Spoerl, E. & Seiler, T. Collagen fiber diameter in the rabbit cornea after collagen crosslinking by riboflavin/UVA. *Cornea* **23,** 503–507 (2004).
72. Galvis, V. *et al.* Keratoconus: an inflammatory disorder? *Eye (London)* **29,** 843–859 (2015).
73. Spoerl, E., Wollensak, G. & Seiler, T. Increased resistance of crosslinked cornea against enzymatic digestion. *Current Eye Research* **29,** 35–40 (2004).
74. Wollensak, G. & Redl, B. Gel electrophoretic analysis of corneal collagen after photodynamic cross-linking treatment. *Cornea* **27,** 353–356 (2008).

75. Cui, L., Huxlin, K. R., Xu, L., MacRae, S. & Knox, W. H. High-Resolution, Noninvasive, Two-Photon Fluorescence Measurement of Molecular Concentrations in Corneal Tissue. *Investigative Ophthalmology and Visual Science* **52,** 2556–2564 (2011).
76. The Beer-Lambert Law. *Chemistry LibreTexts* (2013). Available at: https://chem.libretexts.org/Core/Physical_and_Theoretical_Chemistry/Spectroscopy/Electronic_Spectroscopy/Electronic_Spectroscopy_Basics/The_Beer-Lambert_Law. (Accessed: 9th February 2017)
77. Craig, J. A. *et al.* Epithelium-off photochemical corneal collagen cross-linkage using riboflavin and ultraviolet a for keratoconus and keratectasia: a systematic review and meta-analysis. *The Ocular Surface* **12,** 202–214 (2014).
78. Mazzotta, C. *et al.* Corneal Healing After Riboflavin Ultraviolet-A Collagen Cross-Linking Determined by Confocal Laser Scanning Microscopy In Vivo: Early and Late Modifications. *American Journal of Ophthalmology* **146,** 527–533.e1 (2008).
79. Spoerl, E., Mrochen, M., Sliney, D., Trokel, S. & Seiler, T. Safety of UVA-riboflavin cross-linking of the cornea. *Cornea* **26,** 385–389 (2007).
80. Wollensak, G., Spörl, E., Reber, F., Pillunat, L. & Funk, R. Corneal endothelial cytotoxicity of riboflavin/UVA treatment in vitro. *Ophthalmic Research* **35,** 324–328 (2003).

81. Raiskup, F., Theuring, A., Pillunat, L. E. & Spoerl, E. Corneal collagen crosslinking with riboflavin and ultraviolet-A light in progressive keratoconus: Ten-year results. *Journal of Cataract & Refractive Surgery* **41,** 41–46 (2015).
82. Spoerl, E., Huhle, M. & Seiler, T. Induction of cross-links in corneal tissue. *Experimental Eye Research* **66,** 97–103 (1998).
83. Bunsen-Roscoe law | physics | Britannica.com. Available at: https://www.britannica.com/science/Bunsen-Roscoe-law. (Accessed: 10th February 2017)
84. Schumacher, S., Oeftiger, L. & Mrochen, M. Equivalence of biomechanical changes induced by rapid and standard corneal cross-linking, using riboflavin and ultraviolet radiation. *Investigative Ophthalmology and Visual Science* **52,** 9048–9052 (2011).
85. Wernli, J., Schumacher, S., Spoerl, E. & Mrochen, M. The Efficacy of Corneal Cross-Linking Shows a Sudden Decrease with Very High Intensity UV Light and Short Treatment TimeCorneal Cross-Linking Efficacy. *Investigative Ophthalmology and Visual Science* **54,** 1176–1180 (2013).
86. Shetty, R. *et al.* Current Protocols of Corneal Collagen Cross-Linking: Visual, Refractive, and Tomographic Outcomes. *American Journal of Ophthalmology* **160,** 243–249 (2015).
87. Cingü, A. K. *et al.* Transient corneal endothelial changes following accelerated collagen cross-linking for the treatment of progressive keratoconus. *Cutaneous and Ocular Toxicology* **33,** 127–131 (2014).

88. Turkcu, U. O. *et al.* Protein Oxidation Levels After Different Corneal Collagen Cross-Linking Methods. *Cornea* **35,** 388–391 (2016).

89. Touboul, D. *et al.* Corneal confocal microscopy following conventional, transepithelial, and accelerated corneal collagen cross-linking procedures for keratoconus. *Journal of Refractive Surgery* **28,** 769–776 (2012).

90. Tomita, M., Mita, M. & Huseynova, T. Accelerated versus conventional corneal collagen crosslinking. *Journal of Cataract & Refractive Surgery* **40,** 1013–1020 (2014).

91. Peyman, A., Nouralishahi, A., Hafezi, F., Kling, S. & Peyman, M. Stromal Demarcation Line in Pulsed Versus Continuous Light Accelerated Corneal Cross-linking for Keratoconus. *Journal of Refractive Surgery* **32,** 206–208 (2016).

92. Maurin, C. *et al.* [Assessment of postoperative pain after corneal collagen cross-linking by iontophoresis vs the rapid epithelium-off technique in progressive keratoconus patients]. *Journal Francais D'ophtalmologie* **38,** 904–911 (2015).

93. Wollensak, G. & Iomdina, E. Biomechanical and histological changes after corneal crosslinking with and without epithelial debridement. *Journal of Cataract & Refractive Surgery* **35,** 540–546 (2009).

94. Kissner, A. *et al.* Pharmacological modification of the epithelial permeability by benzalkonium chloride in UVA/Riboflavin corneal collagen cross-linking. *Current Eye Research* **35,** 715–721 (2010).

95. Soeters, N., Wisse, R. P. L., Godefrooij, D. A., Imhof, S. M. & Tahzib, N. G. Transepithelial versus epithelium-off corneal cross-linking for the treatment of progressive keratoconus: a randomized controlled trial. *American Journal of Ophthalmology* **159,** 821–828.e3 (2015).
96. Al Fayez, M. F., Alfayez, S. & Alfayez, Y. Transepithelial Versus Epithelium-Off Corneal Collagen Cross-Linking for Progressive Keratoconus: A Prospective Randomized Controlled Trial. *Cornea* **34 Suppl 10,** S53-56 (2015).
97. Leccisotti, A. & Islam, T. Transepithelial Corneal Collagen Cross-Linking in Keratoconus. *Journal of Refractive Surgery* **26,** 942–948 (2010).
98. Vinciguerra, P. *et al.* Transepithelial Iontophoresis Versus Standard Corneal Collagen Cross-linking: 1-Year Results of a Prospective Clinical Study. *Journal of Refractive Surgery* **32,** 672–678 (2016).
99. Caruso, C. *et al.* Transepithelial Corneal Cross-Linking With Vitamin E-Enhanced Riboflavin Solution and Abbreviated, Low-Dose UV-A: 24-Month Clinical Outcomes. *Cornea* **35,** 145–150 (2016).

CURRICULUM VITAE